EFFECT OF HYDROGEN CONCENTRATION ON VENTED EXPLOSION OVERPRESSURES FROM LEAN HYDROGEN–AIR DEFLAGRATIONS

Bauwens, C.R., Chao, J. and Dorofeev, S.B.
FM Global, Research Division, 1151 Boston-Providence Turnpike, Norwood, 02062, USA,
carl.bauwens@fmglobal.com

ABSTRACT

Experimental data from vented explosion tests using lean hydrogen-air mixtures with concentrations from 12 to 19% vol. are presented. A 63.7-m^3 chamber was used for the tests with a vent size of either 2.7 or 5.4 m^2. The tests were focused on the effect of hydrogen concentration, ignition location, vent size, and obstacles on the pressure development of a propagating flame in a vented enclosure. The dependence of the maximum pressure generated on the experimental parameters was analyzed. It was confirmed that the pressure maxima are caused by pressure transients controlled by the interplay of the maximum flame area, the burning velocity, and the overpressure generated outside of the chamber by an external explosion. A model proposed earlier to estimate the maximum pressure for each of the main pressure transients was evaluated for the various hydrogen concentrations. The effect of the Lewis number on the vented explosion overpressure is discussed.

1.0 INTRODUCTION

Explosion venting is a method commonly used to prevent or minimize damage to an enclosure caused by an accidental explosion. Analytical models and empirical correlations have been developed (see, e.g., [1, 2, 3]), to estimate the vent size requirements for specific locations. In these models, a single reduced-peak pressure is expressed in terms of a vent parameter that describes the competition between the increase of gas volume caused by combustion and the loss of gas volume due to venting. Engineering safety standards, such as NFPA 68, use these correlations in order to estimate the appropriate vent size for a given practical scenario [4].

The current vent size correlations, however, can often have conflicting recommendations depending on the specific scenario being considered. A range of factors can affect the pressure development of a propagating flame in a vented enclosure, particularly, the enclosure size and geometry, vent size, vent deployment pressure, ignition location, and the presence of obstacles. The models currently in use only estimate a single overall reduced-peak overpressure and do not take into consideration the different effects and relative importance of these various factors.

Furthermore, it has been shown experimentally that more than one distinct pressure transient is generated as a result of the venting process and the magnitude of each pressure transient is governed by different physical mechanisms [5, 6, 7]. In the case of lean hydrogen-air mixtures, additional factors must be examined. In particular, the contribution of thermal-diffusive flame instabilities that are present in lean hydrogen flames must be included; otherwise, correlations using the laminar flame speed alone can significantly under predict the overpressures generated.

The objective of the present study is to examine the effect of hydrogen concentration on vented explosions for lean hydrogen-air mixtures. Experimental data for mixtures of varying concentration, from 12% to 19% by volume, are presented and the effect of hydrogen concentration on the flame velocities and overpressures generated is examined as well as the effect of the Lewis number (*Le*) of the mixture. In addition, the experimental results are compared with a previously developed model for predicting peak overpressures and the performance of this model is evaluated.

2.0 BACKGROUND

In the recent studies [6, 7], vented explosions under various experimental conditions were systematically investigated using multiple pressure and flame speed measurements that were synchronized with high-speed videos. From these studies, three main pressure transients were identified that can be responsible for the maximum the overall peak overpressure and the specific pressure transient that is the strongest is highly dependent on the initial conditions. These three pressure peaks were associated with the external explosion (P_{ext}), flame-acoustic interactions as the flame approaches the chamber walls (P_{vib}) and an increase in flame surface area associated with the presence of obstacles (P_{obs}).

A parametric study was undertaken to examine the effects of ignition location, mixture composition, vent size, blockage due to obstacles, and scale on the three different pressure transients observed during a vented explosion [6, 7, 8, 9, 10]. No global trend was discernible, although the individual relationships between each pressure peak and each of these factors were identified.

In addition to the factors listed above, the effect of thermal-diffusive flame instabilities plays a critical role in lean hydrogen-air mixtures. In previous studies examining 18% vol. hydrogen-air mixtures [10], the measured burning velocity in vented explosion tests was found to be approximately twice the laminar value due to thermal-diffusion effects.

In order to combine the data, a simple model was proposed to estimate the magnitude of each individual pressure peak which was then compared to the experimental results for stoichiometric propane–air mixtures [11]. This model was further extended to different fuels, enclosure sizes and additional experimental results previously reported by other investigators [12].

3.0 EXPERIMENTAL SETUP

The data presented here were obtained from experiments performed in a 63.7 m^3 explosion test chamber with overall dimensions of 4.6 x 4.6 x 3.0 m. A square vent was used in all tests, with an area of either 5.4 or 2.7 m^2, which was located on one of the vertical walls. Overpressure was measured using four pressure transducers at different locations inside the chamber mounted to the chamber walls (see Fig. 1). Flame time-of-arrival thermocouples were used to measure flame velocity as a function of distance. The thermocouples were located at a height of 1.4 m above the floor of the chamber and were placed at 0.5 m intervals inside the chamber and at 1 m intervals outside of the chamber. External pressure was measured using two blast-wave pressure transducers mounted to a concrete slab outside of the chamber, below the line of thermocouples at a height of 0.3 m above the ground, 1.17 and 3.45 m from the vent. The experimental data was acquired at a sampling rate of 25,000 scans/sec.

In this study, hydrogen-air mixtures with compositions varying in the range 12-19% vol. were examined. The initial mixture was created by injecting 99.9% hydrogen through an inlet at the center of the floor of the chamber while mixing fans within the chamber were used to create a uniform mixture. The concentration of gas inside the chamber was controlled using a Cirrus mass spectrometer. Prior to ignition and during mixing, the unburned mixture was contained within the chamber using a sheet of polypropylene with a thickness of 0.02 mm. Ignition was supplied using a carbon rod igniter at one of three locations, either at the center of the chamber, 0.25 m from the center of the wall opposite the vent (back ignition) or 0.25 m from the center of the wall containing the vent (front ignition). The initial turbulent intensity was controlled by maintaining a fixed time between when mixing fans were stopped and ignition, producing a turbulent intensity of $u' \approx 0.1$ m/s, which was measured in a series of preliminary tests using measurements from a bi-directional velocity probe.

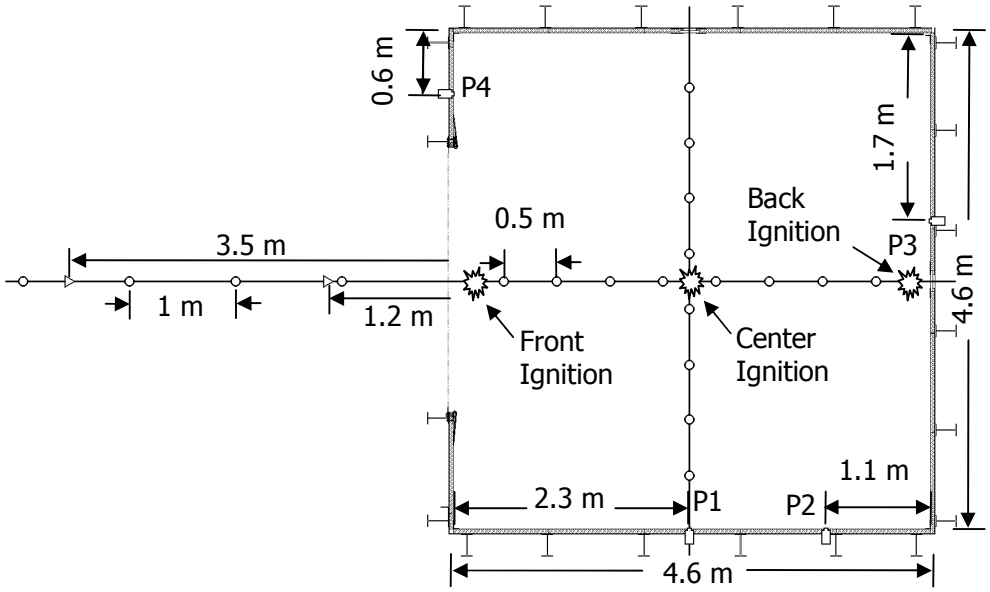

Figure 1. Top view of the chamber, showing the locations of pressure transducers, (rectangles), flame arrival thermocouples (circles), blast-wave pressure transducers (triangles) and the three ignition locations.

4.0 EXPERIMENTAL RESULTS

Table 1. Summary of Experimental Results and Flame Properties

Test	Ign. Loc.	Vent Size (m^2)	Obs.	Conc. (±0.3%)	S_L (m/s)	σ	Lewis Number	P_{ext} (bar)	P_{vib} (bar)
1	CI	5.4	0	12.1	0.22	3.95	0.38	0.008	0.009
2	CI	5.4	0	14.9	0.37	4.54	0.42	0.020	0.016
3	CI	5.4	0	18.0	0.64	5.15	0.46	0.071	0.042
4	CI	5.4	0	18.1	0.65	5.16	0.46	0.061	0.040
5	CI	5.4	0	19.1	0.77	5.36	0.48	0.108	0.067
6	CI	5.4	0	19.7	0.85	5.48	0.49	0.111	0.076
7	CI	2.7	0	17.5	0.59	5.06	0.46	0.112	0.228
8	CI	2.7	0	18.0	0.64	5.15	0.46	0.124	0.234
9	CI	5.4	8	15.8	0.44	4.73	0.43	0.040	-
10	CI	5.4	8	18.3	0.68	5.22	0.47	0.094	-
11	CI	5.4	8	18.5	0.70	5.25	0.47	0.089	-
12	BW	5.4	0	17.2	0.56	4.99	0.45	0.130	0.046
13	BW	5.4	0	17.9	0.64	5.14	0.46	0.150	0.06
14	BW	5.4	0	18.3	0.68	5.21	0.47	0.125	0.016
15	BW	2.7	0	15.1	0.39	4.59	0.42	0.127	0.066
16	BW	2.7	0	17.1	0.55	4.97	0.45	0.247	0.115
17	BW	2.7	0	17.8	0.63	5.12	0.46	0.314	0.228
18	BW	5.4	8	18.1	0.65	5.16	0.46	0.428	-
19	FW	5.4	0	18.2	0.67	5.19	0.47	-	0.038
20	FW	2.7	0	18.0	0.64	5.15	0.46	-	0.171
21	FW	5.4	8	18.3	0.68	5.22	0.47	-	-

The experimental results presented here are a combination of existing test data from previous studies [11, 12] with additional tests performed at different concentrations. The results of the tests are summarized in Table 1, along with values for the mixture properties used in the model for each concentration. The table summarizes the test configuration including: ignition location (Ign. Loc.), vent size, obstacle configuration (Obs.), concentration (Conc.), laminar burning velocity (S_L), expansion ratio (σ), the Lewis Number and the peak pressures generated due to the external explosion (P_{ext}) and flame acoustic interactions (P_{vib}). In this study, the pressure peak due to the maximum flame area (P_{obs}) was not examined as there was insufficient data with respect to the different concentrations.

Figure 2 shows the laboratory frame velocity of the flame as a function of distance from ignition. The figure illustrates how the velocity of the flame increases with the concentration of the mixture and is consistent with the increase in laminar burning velocity and expansion ratio of the mixtures.

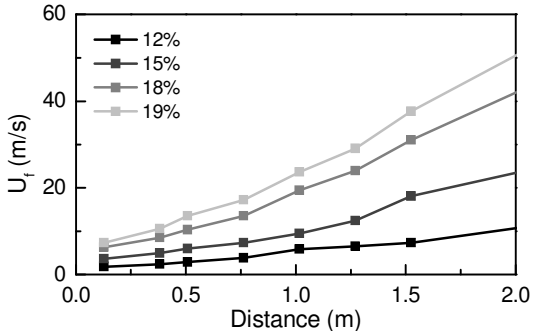

Figure 2. Laboratory frame velocity plots comparing different concentrations for center ignition hydrogen-air explosions with a 5.4 m^2 vent.

When the velocities are normalized by the product of expansion ration and laminar burning velocity (σS_L) of the mixture, see Fig. 3, the velocity-distance profiles nearly collapse to a single curve. The initial flame speed is still higher than laminar flame speed, however, due to thermal-diffusive effects. To estimate the increase in burning velocity due to these effects, the following relation was used:

$$\Xi_{Le} = 0.9Le^{-1} \tag{1}$$

where Ξ_{Le} is the increase in burning velocity due to thermal-diffusive effects and *Le* is the Lewis Number of the mixtures. This relation was found through fitting against the initial flame speeds measured in the tests. The exponent of -1 is similar to that obtained in a study by Driscoll [13] with an additional coefficient of 0.9 added to match the factor of $\Xi_{Le} = 2$ for 18% hydrogen-air mixtures found in the previous studies [10]. When corrected by the factor Ξ_{Le}, the normalized curves further collapse to a single curve and the initial velocity of the curves normalize to one illustrating how this factor captures the increased burning velocity due to the thermal-diffusive instability.

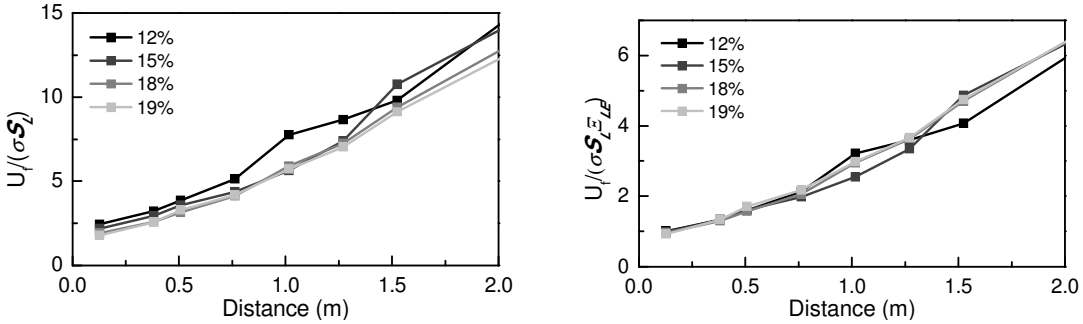

Figure 3. Normalized velocity plots comparing different concentrations for center ignition hydrogen-air explosions with a 5.4 m^2 vent

Figure 4 shows a comparison of pressure-time histories for center ignition hydrogen-air explosions with a 5.4 m^2 vent over a range of concentrations from 12% to 19%. The figure shows both 80 Hz low-pass and 80 Hz high-pass filtered results. The low-pass filtered results correspond to potentially damaging overpressures, while the higher frequency pressure oscillations lack sufficient impulse to cause damage to most structures. As to be expected, the lower concentration mixtures produced lower overall peak (low-pass filtered) pressures, due to the lower flames speed and the expansion ratio. It is interesting to note, however, that the amplitude of the high frequency (>80Hz) component of the pressure traces increased with lower concentration. This increase may be due to increased coupling between the flame-acoustic oscillations due to increased thermal-diffusion effects or to the fact that the lower flame-speed of the leaner mixtures allows the oscillations to grow in amplitude for a longer time before the flame reaches the walls of the chamber. The increased amplitude of pressure oscillations did not result in higher low frequency overpressures, indicating that any increase in the flame speed due to an increase in amplitude of the high frequency acoustics did not overcome the reduction in burning velocity due to the lower concentration. This result may, however, have implications on any model or correlation used to predict P_{vib}. If the amplified flame-acoustic interactions at lower concentrations lead to an increase in burning velocity, then the model would have to take this into account. Otherwise, the model would under predict the flame speed during the acoustic oscillations for leaner mixtures and over predict for lean mixtures closer to stoichiometric.

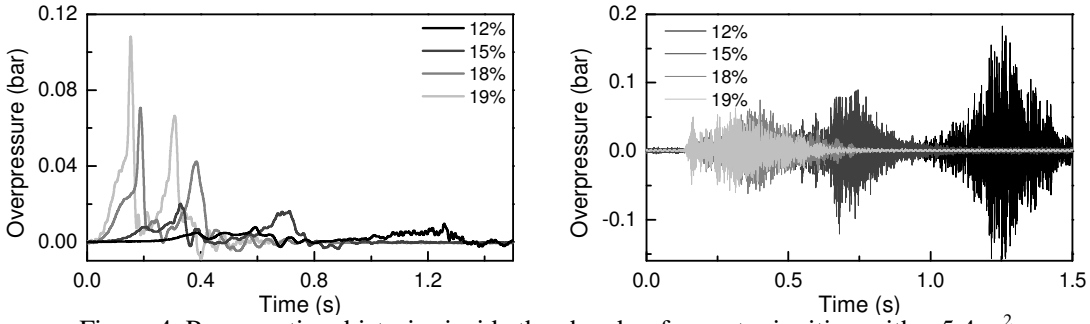

Figure 4. Pressure-time histories inside the chamber for center ignition with a 5.4 m^2 vent. Filtered by an 80 Hz low-pass filter (left) and an 80 Hz high-pass filter (right).

5.0 MODEL FOR OVERALL PEAK PRESSURE

The development of a general correlation for vent sizing is complicated by the fact that the overall peak overpressure can be caused by any one of the three main pressure transients, each of which is governed by different physical mechanisms. These individual pressure peaks, however, can each be evaluated using a principle similar to previous simplified analytical models [1-3]. The present model has been described in detail in previous work [11, 12]; thus only the important expressions from the model and the general rationale behind them are outlined briefly in the present paper.

The maximum overpressure achieved during vented explosions occurs when the production of combustion products due to a flame propagating is equal to the rate of venting:

$$\frac{p}{p_0} = \frac{p_e}{p_0}\left(1 - G\left(\frac{S_u A_f(\sigma-1)}{a_{cd}A_v}\right)^2\right)^{-1} = \frac{p_e}{p_0}\left(1 - G/A_v^{*2}\right)^{-1} , \quad (2)$$

where p, A, A_v^*, and S_u are pressure, area, vent parameter and the burning velocity relative to the unburned mixture. The subscripts 0, *e*, *f*, and *v* denote ambient, external, flame and vent conditions. The coefficient G is a constant for each mixture related to the ratio of specific heats, γ. The parameter a_{cd} is related to the flow exiting the vent and is a function of the properties of the gas being vented and the discharge coefficient of the vent. Equation (2) can be used to illustrate how the different factors are responsible for peak overpressures in a vented enclosure. An increase to the external pressure, p_e, due to an external explosion results in a corresponding internal pressure increase and the

development of pressure peak P_{ext}. The increase in the burning velocity, S_u, due to flame-acoustic interactions creates pressure peak, P_{vib}. The growth of the flame area, A_f, due to obstacles is responsible for the pressure peak, P_{obs}. Use of this model, either for comparison with experimental data or for vent sizing applications, requires estimates for the maximum flame area, the burning velocity, and the external explosion overpressure.

5.1 Maximum Flame Area

5.1.1 P_{ext} and P_{vib} without obstacles

Predicting pressure peaks, P_{ext} and P_{vib} requires estimates for both the flame surface area at the time of the pressure transient as well as the burning velocity. This surface area depends on the ignition location within the chamber.

For calculating P_{ext} the flame surface area when the flame exits the chamber is needed. For back ignition the shape of the flame can be approximated as an ellipsoid twice the length of the chamber with the same height and width of the chamber. For center ignition, the flame is assumed to propagate spherically with a correction for the non-symmetric propagation due to the presence of the vent. There is assumed to be no external explosion peak with front ignition due to the limited quantity of unburned gas that is vented.

Pressure peak, P_{vib}, occurs when the flame approaches the walls of the chamber. Thus, for P_{vib} the maximum flame area is estimated to be 0.9 times the surface area of the internal chamber walls, A_{cw}, minus the area where products are in contact with the walls or the vent.

5.1.2. Effect of obstacles on P_{ext} and P_{obs}

The presence of obstacles increases the surface area of the flame and must be considered. A spherical flame propagating through obstacles may be estimated from the ratio of the flame area with obstacles to the flame area without obstacles [14, 15],

$$\frac{A_f}{A_{f0}} = \left(1 + 4/3 \cdot \sigma^{1-\alpha}(BR)^{1/2}N^{\alpha}\right)^2, \tag{3}$$

where BR is the average area blockage provided by the obstacles, N is the average number of layers of obstacles in the flame path, and $\alpha = 0.63$. The obstacle configuration used in this study was a 2x4 array of square cross-section obstacles arranged parallel to the vent. Thus for back-wall ignition, this model is applied with $N = 2$; for center ignition, $N = 0.5$ because only the portion of the flame surface propagating towards the vent is effectively increased by the obstacles due to volume expansion. By the same rationale, $N = 0$ is used for front-wall ignition.

5.2. Burning velocity

In a previous study [10], it was found that flame-speed histories can be scaled by their initial flame speeds. According to the experimental data, the initial-burning velocities, S_{u0}, for propane–air and methane–air were measured to be close to the laminar values of $S_L = 0.4$ and 0.38 m/s, respectively. For lean hydrogen–air, however, the burning velocity was found to be higher than the laminar value due to thermal-diffusion effects; thus, $S_{u0} = \Xi_{Le}S_L$. For 18% hydrogen-air mixtures, a value of $\Xi_{Le} = 2$ was used as an effective value.

During the pressure transients P_{ext} and P_{obs}, it may be assumed that $S_u \approx S_{u0}$ and that any deviation is included in the estimate of the flame area, A_f. For the pressure transient, P_{vib}, however, a significant increase of the burning velocity is observed in experiments due to flame–acoustic interactions. In the model this effect is treated by introducing a constant flame-wrinkling factor, Ξ_A, such that $S_u = \Xi_A S_L$, which is fitted to match the experimental results.

5.3. Overpressure generated by the external explosion

The maximum overpressure due to flame propagation in a cloud of radius, R_e (with a volume equal to the flame volume in an enclosure just as the flame reaches the vent) is given by [14, 15]:

$$\frac{p_e}{p_0} - 1 = \frac{\gamma(\sigma-1)S_u}{4\pi a_0^2 \sigma R_e}\frac{d}{dt}\Big(S_u(t)A_f(t)\Big). \tag{4}$$

The time derivative on the right-hand side of Eq. (4) may be considered the result of two factors: the growth of a spherical flame brush and the change in a flame-wrinkling factor, Ξ, due to turbulence or flame instabilities. It has been shown that Rayleigh–Taylor instability plays an important role in flame acceleration during an external explosion [10]. As the flame propagates through the vent and the vented reactants become products, the volumetric-venting rate increases proportionally to a_{cd} and leads to an acceleration, a, in the Rayleigh–Taylor unstable direction.

The value of Ξ can be determined by the rate of surface-area generation due to the instability and to the removal rate due to flame propagation. For simplicity, Ξ can be taken to grow linearly with time such that $\Xi(t) = 1 + \Xi_0 t$. The constant $\Xi_0 = (k_T a)^{1/2}$ is proportional to the generation rate of the Rayleigh–Taylor instability, and k_T [1/m] is estimated from the experimental data. Thus, the following expression for the overpressure of the external explosion can be used (for $\Xi_0 t \gg 1$):

$$\frac{p_e}{p_0} - 1 = \frac{20\gamma(\sigma-1)\sigma S_u R_e\sqrt{k_T a}}{a_0^2} \tag{5}$$

6. DISCUSSION

Figure 5 shows a comparison of the pressure peak P_{ext} observed in the tests with the results of the model. In general, good agreement was found between the model and experimental results. The difference between using a constant $\Xi_{Le} = 2$ factor and one that varies with Lewis number was not significant, although there is a slight improvement in the performance of the correlation with a variable Ξ_{Le}. This slight difference is due to the small variation in *Le* over the range of concentrations studied. It is likely that concentrations closer to stoichiometric, with significantly larger *Le*, would be over-predicted by the model if the constant value of $\Xi_{Le} = 2$ were used.

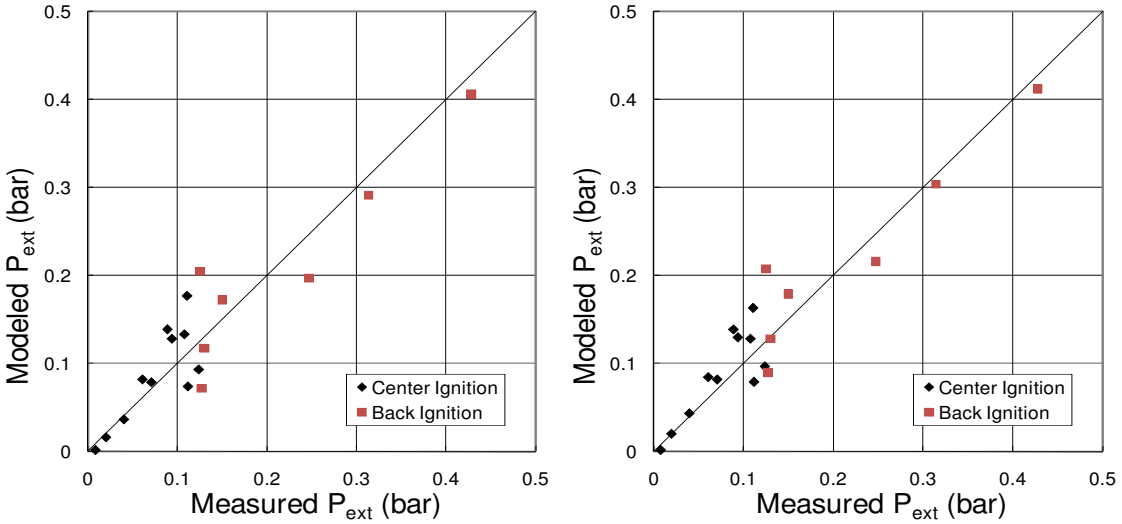

Figure 5. Modeled vs measured P_{ext}, constant Ξ_{Le} (left) and with $\Xi_{Le} = 0.9Le^{-1}$ (right)

When the results are compared with the flame-acoustic peak P_{vib}, see Fig. 6, similar results are obtained. There is more scatter in the results for this peak, due to the inherent scatter of the data obtained in experiments. Introducing the variable Ξ_{Le} coefficient does improve the results more for

P_{vib} than for P_{ext}, however, the difference is still not significant compared to the scatter of the data. These results indicate that for the range of hydrogen concentrations 12-19% a constant value of $\Xi_{Le} = 2$ is adequate for the purpose of predicting the overpressure.

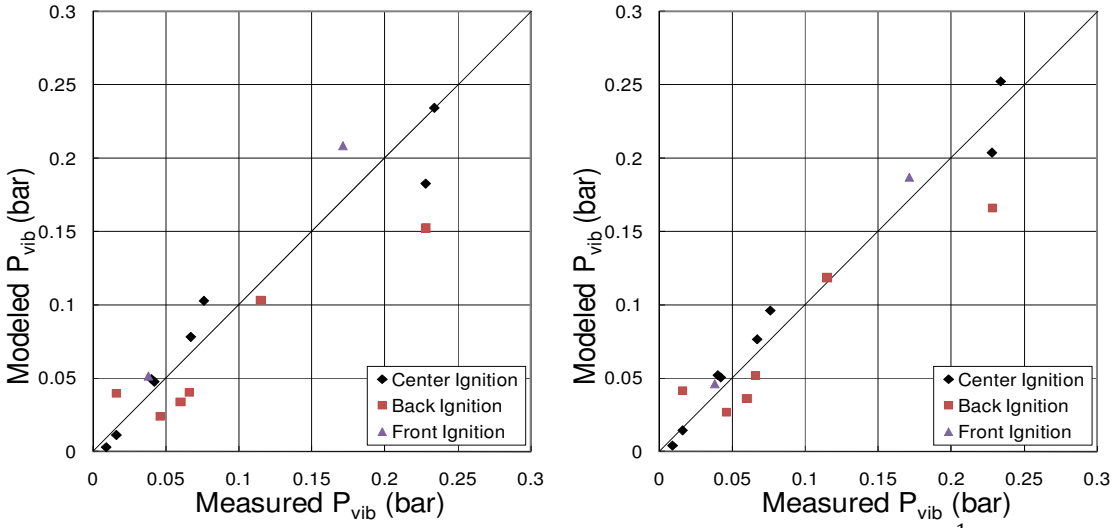

Figure 6. Modeled vs measured P_{vib}, constant Ξ_{Le} (left) and with $\Xi_{Le} = 0.9Le^{-1}$ (right)

The agreement between the model results and the experimental data is based on several assumptions used in the model and two model constants, Ξ_A and k_T, that were determined to fit the data. The assumptions used, such as estimating the maximum flame area to be 0.9 of the respective area of the chamber walls, are relatively well grounded and it can be argued that their relative uncertainty is of the order of 10%. An important observation that follows from this study is that with a single set of reasonable assumptions and only two empirical constants the model was able to reproduce the correct trends for pressure transients over a wide range of initial conditions with variable ignition locations and vent size and obstacles.

7. CONCLUSION

Results of vented explosion tests obtained in a room-size enclosure with and without obstacles for a range of hydrogen-air mixtures from 12 to 19% vol. have been presented. It was found that the main physical phenomena responsible for pressure generation under this range of initial conditions were the same as those seen in previous studies and that three physical phenomena were mainly responsible for the overall peak pressure rise observed during a vented explosion. In general, it was found that the strength of the pressure transients is defined by the interplay of various factors such as the maximum flame area and burning velocity in the chamber and the overpressure generated by the external explosion. These factors, in turn, depend on the ignition location, obstacles and vent size and the relative strength of each pressure peak varies with the test configuration.

It was also found that peak pressures were reduced when hydrogen concentrations, and hence the burning velocity of the flame, were reduced. The high frequency component of the pressure-time profiles increased with decreasing hydrogen concentration but this effect was not sufficient to overcome the difference in burning velocity between mixtures and did not produce significant differences in the lower frequency overpressures. When normalized by the burning velocity and expansion ratio, the velocity-distance profiles between different concentrations scaled well and the introduction of an additional factor Ξ_{Le} slightly improved the agreement.

Comparing the experimental results to the previously developed model for predicting peak overpressure found good agreement between model and experiments, typically to within the uncertainty of the experimental data. Incorporating an additional relationship between the *Le* number

and thermal-diffusive flame instabilities slightly improves performance of the correlation, particularly for P_{vib}. However, the difference is not significant due to the relatively small variation of *Le* over the range of concentrations studied. At high concentrations, closer to stoichiometric, the coefficient would produce a stronger effect and including its variability may be necessary to maintain good agreement between the model and experimental results.

ACKNOWLEDGEMENTS

The work presented in this paper was funded by FM Global and performed within the framework of the FM Global Strategic Research Program on Explosions and Material Reactivity. The authors are thankful to Franco Tamanini for many helpful discussions of the measurement techniques and test results. The technical assistance of Mike Gravel and Kevin Mullins in preparing and conducting the tests is greatly appreciated.

REFERENCES

1. D. Bradley and A. Mitcheson, The Venting of Gaseous Explosions in Spherical Vessels, *Combust. Flame* **32**, 1978, pp. 221-255.
2. V.V. Molkov, R. Dobashi, M. Suzuki and T. Hirano, Modeling of Vented Hydrogen-Air Deflagrations and Correlations for Vent Sizing, *J. Loss Prev. Process*, **12**, 1999, pp. 147-156.
3. F. Tamanini, Scaling Parameters for Vented Gas and Dust Explosions, *J. Loss Prev. Process,* **14**, 2001, pp. 455.
4. NFPA 68, Standard on Explosion Protection by Deflagration Venting, 2007 Edition, National Fire Protection Association, Quincy, MA 02269, 2007.
5. M.G. Cooper, M. Fairweather and J.P. Tite, On the Mechanisms of Pressure Generation in Vented Explosions, *Combust. Flame*, **65**, 1986, pp. 1-14.
6. C.R. Bauwens, J. Chaffee and S.B. Dorofeev, Experimental and Numerical Study of Methane-air Deflagrations in a Vented Enclosure, Sixth International Symposium on Fire Safety Science, September, 2008, Germany.
7. C.R. Bauwens, J. Chaffee and S.B. Dorofeev, Experimental and Numerical Study of Hydrogen–air Deflagrations in a Vented Enclosure, Sixth International Symposium on Hazards, Prevention and Mitigation of Industrial Explosions, 2008, St. Petersburg, Russia.
8. D.P.J. McCann, G.O. Thomas and D.H. Edwards, Gasdynamics of Vented Explosions Part I: Experimental Studies. *Combust. Flame*, **59**(3), 1985, pp. 233-250.
9. R.G. Zalosh, Gas Explosion Tests in Room-Size Vented Enclosures, Proceedings of the 13th Loss Prevention Symposium, 1979, Houston, pp. 98-108.
10. C.R. Bauwens, J. Chaffee and S.B. Dorofeev, Vented Explosion Overpressures from Combustion of Hydrogen and Hydrocarbon Mixtures, *J. Hyd. Energy*, **36**(3), 2011, pp. 2329.
11. C.R. Bauwens, J. Chaffee and S.B. Dorofeev, Effect of Ignition Location, Vent Size and Obstacles on Vented Explosion Overpressure in Propane-Air Mixtures. *Combust. Sci. Tech*, **182**(11), 2010, pp. 1915.
12. J. Chao, C.R. Bauwens and S.B. Dorofeev, An Analysis of Peak Overpressures in Vented Gaseous Explosions, *Proc. Comb. Inst.*, **33**(2), 2011, pp. 2367.
13. J.F. Driscoll, Turbulent Premixed Combustion: Flamelet Structure and Its Effect on Turbulent Burning Velocities, *Prog. Energ. Combust.*, **34**, 2008, pp. 91-134.
14. R.A. Strehlow, Blast Wave from Deflagrative Explosions: An Acoustic Approach, in: 13th AIChE Loss Prevention Symposium, Philadelphia, USA, 1981.
15. W.E. Baker, P.A. Cox, P.S. Westine, J.J. Kulesz and R.A. Strehlow, Explosion Hazards and Evaluation, Elsevier, Amsterdam, Oxford, New York, 1983.